Title: Differences in Anatomical Connections across Distinct Areas in the Rodent Prefrontal Cortex

Running title: Anterior-posterior organisation of PFC connections

Authors: Stacey A Bedwell[1], E Ellen Billett[1], Jonathan J Crofts[1], Chris J Tinsley[1]

Corresponding author: Chris Tinsley

Address #1:
School of Science and Technology
Nottingham Trent University
Clifton Lane
Nottingham
NG11 8NS

Number of pages: 22

Number of figures: 10

Number of tables: 1

Number of words (abstract): 202

Number of words (introduction): 585

Number of words (discussion): 1227

Number of words (whole manuscript): 4588

Conflicts of Interests:

The authors declare no conflict of interests

Acknowledgements

This work was supported by a Nottingham Trent University studentship awarded to Stacey Bedwell. We would like to thank Andrew Marr and Danielle MacDonald for their technical support.

Abstract

The organisation of connections is typically ordered throughout the cerebral cortex. Studies of the Prefrontal Cortex (PFC) have indicated that its connections are also ordered. Here we injected Fluoro-Gold and Fluoro-Ruby into the same sites throughout rat PFC. Tracer injections were applied to 2 coronal levels within the PFC (anterior +4.7mm to bregma; central and posterior +3.7mm to bregma). Within each coronal level tracers were deposited at sites separated by approximately 1mm and located parallel to the medial and orbital surface of the cortex. Following the injections we found that both Fluoro-Gold and Fluoro-Ruby produced prominent labelling in temporal and sensory-motor cortex. Fluoro-Gold produced retrograde labelling and Fluoro-Ruby largely produced anterograde labelling. Analysis of the location of these connections within temporal and sensory-motor cortex revealed consistent topological ordering (as the sequence of injections was followed mediolaterally along the orbital surface of each coronal level). At the anterior coronal level, injections produced a similar pattern of ordering to that seen in central PFC in earlier studies from our laboratory (i.e. comparing equivalently located injections employing the same tracer), this was particularly prominent within temporal cortex. However, at the posterior coronal level this pattern of ordering differed in both temporal cortex and sensory-motor cortex.

Rat prefrontal cortex (PFC) is known to be crucially important in mediating a variety of cognitive (Alvarez and Emory, 2006; Fuster, 2001; Kolb, 1984; Schoenbaum and Roesch, 2005) and autonomic functions (Neafsey, 1990; Frysztak and Neafsey, 1994) yet it's anatomical structure is still not entirely described. In the rat brain prefrontal cortex is divided into distinct cytoarchitectural divisions within a broader grouping of medial and orbital PFC. Medial PFC includes the prelimbic (PL), infralimbic (IL) and anterior cingulate regions (Vertes, 2004; Vertes, 2006). Orbital PFC contains medial orbital (MO), ventral orbital (VO), ventral lateral orbital (VLO) and lateral orbital (LO) regions (Krettek and Price, 1977; Van De Werd and Uylings, 2008). The dorsal lateral orbital region (DLO) lies between LO and the agranular insular area (Van De Werd and Uylings, 2008). Medial PFC (mPFC) and orbital PFC are proposed to be functionally distinct (Schoenbaum and Roesch, 2005; Schoenbaum and Esber, 2010) and both regions are known to display different connections to other brain sites. Medial PFC is known to have important roles in the timing of motor behaviours (Narayanan and Laubach, 2006; Narayanan and Laubach, 2008; Narayanan and Laubach, 2009; Smith et al., 2010; Kim et al., 2013) and orbital PFC is proposed to provide information in terms of the expected outcomes of events (Schoenbaum and Esber, 2010; Schoenbaum and Roesch, 2005; Stalnaker et al., 2015).

Anatomical studies have reported topologically ordered projections from PFC to temporal and sensory-motor regions in rats (Sesack et al., 1989; Vertes, 2004; Hoover and Vertes, 2011; Kondo and Witter, 2014; Bedwell et al., 2014; Bedwell et al., 2015). Further topologically ordered connections have been reported in the projections from temporal cortex and sensory-motor cortex to PFC (Delatour and Witter, 2002; Bedwell et al., 2014; Bedwell et al., 2015; Reep et al., 1996). Ordering of connections from PFC to subcortical regions has also been described in the connections from PFC to the striatum (Berendse et al., 1992; Schilman et al., 2008). Taken together these studies provide strong evidence for ordered PFC connections. Within a wider context of brain connectivity this is entirely consistent because there is evidence that both sensory-motor cortex (Porter and White, 1983; Aronoff et al., 2010; Henry and Catania, 2006) and temporal cortex (Delatour and Witter, 2002; Arnault and Roger, 1990; Burwell et al., 1995) contain topographically ordered connections to other brain regions.

Typically, the ordering of PFC connections has often been described along the medial lateral axis of the PFC. Changes in the organisation of rat cingulate PFC connections along the

anterior-posterior (A-P) axis have also been identified (Olson and Musil, 1992). It is unclear whether or not this is a wider organisational principle also present in other regions of PFC or what the precise functional relevance of such an organisation might be. However, it has been proposed that there are changes in cognitive processing characteristics such as abstraction in anterior compared to posterior prefrontal cortex in humans (Taren et al., 2011).

The current study aimed to establish how the organisation of connections changes between anterior and posterior PFC. The neuronal tracers Fluoro-Gold and Fluoro-Ruby were injected into regions of medial and lateral PFC (PL, VO, VLO and DLO). We found that anterior and posterior PFC showed clear ordering in the connections to temporal and sensory-motor cortex. Our findings show that the ordering observed and the relationship between input and output connections changes between anterior and posterior PFC regions, this was clearest in the connections to temporal cortex.

Experimental Procedures

Data was collected from 14 male CD rats (296-367g, Charles River, UK). Animal procedures were carried out in accordance with the UK Animals scientific procedures act (1986), EU directive 2010/63 and were approved by the Nottingham Trent University Animal Welfare and Ethical Review Body. On receipt the animals were examined for signs of ill-health or injury. The animals were acclimatized for 10 days during which time their health status was assessed. Prior to surgery the animals were housed together in individually ventilated cages (IVC; Techniplast double decker Greenline rat cages). The animals were allowed free access to food and water. Mains drinking water was supplied from polycarbonate bottles attached to the cage. The diet and drinking water were considered not to contain any contaminant at a level that might have affected the purpose or integrity of the study. Bedding was supplied by IPS Product Supplies Ltd in the form of 8/10 corncob. Environmental enrichment was provided in the form of wooden chew blocks and cardboard fun tunnels (Datesand Ltd., Cheshire, UK). Post-surgery the animals were individually or pair housed in the same conditions. The animals were housed in a single air-conditioned room within the Biological support facilities barrier unit, Nottingham Trent University. The rate of air exchange was at least fifteen air changes per hour and the low intensity fluorescent lighting was controlled to give 12 h continuous light and 12 h darkness. The temperature and relative

humidity controls were set to achieve target values of 21 ± 2°C and 55 ± 15% respectively.

Individual bodyweights were recorded on Day - 10 (prior to the start of dosing) and daily thereafter. All animals were examined for overt signs of ill-health or behavioral change immediately prior to surgery dosing, during surgery and the period following surgery. There were no observed clinical signs/symptoms of toxicity or infection. There was no significant effect on body weight development detected.

Rats were anaesthetized with isoflurane (Merial, Harlow, UK) and placed in a stereotaxic frame with the incisor bar set so as to achieve a flat skull. Buprenorphine (0.05 mg/kg i.m/s.c) and Meloxicam (up to 1 mg/kg s.c/orally) analgesia were provided peri-operatively and for several days post-operatively. Body temperature was monitored during and immediately after surgery using a rectal thermometer. Craniotomies (<1 mm) were made at predetermined stereotaxic coordinates. Sterile tracer solution was deposited into the PFC via a 0.5 µl neuro-syringe (Hamilton, Germany).

Injections of anterograde (10% Fluoro-Ruby in distilled water, Fluorochrome, Denver, Colorado (10 nl/min, 2 min diffusion time)) and retrograde tracer (4% Fluoro-Gold in distilled water, Fluorochrome, Denver, Colorado (100 nl/min, 2 min diffusion time)) were made into anterior, central and posterior PL, VO, VLO or DLO with the intention of revealing the anatomical connections of prefrontal regions. The distance between craniotomy co-ordinates (1 mm) was based on the measured spread of tracers in preliminary and previous studies (<1 mm in diameter). Craniotomies were repeated at 2 anterior-posterior levels (+4.2mm and +3.2mm from Bregma) – see full list of animals and corresponding injection sites in table 1. The medial-lateral co-ordinates and depth of injections below the cortical surface at the anterior and posterior levels are shown in Figure 1. Figure 1 shows that the histological assessed locations of the injections differed slightly from the surgical coordinates, i.e. the anterior and posterior injections were assessed as occurring wat +4.7mm and +3.7mm with respect to bregma and following the atlas of Paxinos and Watson, 1998.

Each rat received injections of Fluoro-Ruby (100nl) and/or Fluoro-Gold (100nl) into various subdivisions of PFC, separated by 1 mm. Rats received an injection of Fluoro-Gold into one hemisphere and an injection of Fluoro-Ruby into the other hemisphere to allow accurate identification of the tracers injected.

Following a survival time of 7–9 days, the rats were deeply anesthetized with pentobarbital (Sigma-Aldrich, UK), and transcardially perfused with phosphate buffered saline (PBS) (pH 7.4) (~200 ml) followed by 4% paraformaldehyde (PFA) (pH 7.4) (~200 ml). The brain was subsequently removed and stored for 24 h in 4% PFA in PBS (pH 7.4), followed by cryoprotection in 30% sucrose in PBS.

Anatomical processing

For analysis of connections, two series of 40µm coronal sections were taken (2 in 6 sections) on a freezing microtome (CM 1900, Leica, Germany). Sections were mounted onto gelatin coated slides. The first series was cover slipped with Vectashield® mounting medium (with propidium iodide) for fluorescent imaging of Fluoro-Gold (for the injection site and labelling). A parallel series of 40µm coronal sections was cover slipped with Vectashield® mounting medium (with DAPI) for fluorescent imaging of Fluoro-Ruby (for the injection site and labelling).

Sections were examined using fluorescent microscopy (Fluoro-Ruby and Fluoro-Gold). Fluorescent photos were captured of the injection sites and labels using an Olympus DP-11 system microscope with a x4, x10 and x20 objective lens.

Immunofluorescent labelling of alpha tubulin with fluorescein enabled us to visualize where Fluoro-Ruby labelling occurred in relation to cell bodies, thus establishing the anterograde/retrograde nature of Fluoro-Ruby. Alpha-Tubulin was labelled in several animals R37, R38 and R39. Sections were incubated in an alpha-tubulin monoclonal primary antibody (sc-398103, Santa Cruz, TX) at a dilution of 1:50 overnight at 4ºC and secondary antibody (Fluorescein Horse Anti-Mouse IgG Antibody, Vector Laboratories, UK (in PBS, 2% NS) at a dilution of 1:75 for 1-2 hours. Fluorescein labelled sections were cover-slipped with Vectashield® mounting medium (with DAPI) for fluorescent imaging. Fluoro-Ruby labels, DAPI labelled nuclei and fluorescein labeled α-Tubulin were visualized at a high resolution using confocal microscopy.

Microscopic analysis

The entire forebrain was examined for labelling. Areas of temporal and sensory-motor cortex were found to contain the strongest and most consistent

labelling of connections from anterior and posterior PFC. A more detailed analysis was carried out on these regions to examine the organisation of connections across PFC.

Alpha-tubulin and Fluoro-Ruby labelling was visualised with confocal microscopy. A Z-series of images was taken at X10, X20 and X40 magnification in sequential scanning mode for each channel using Leica confocal software (LAS AF). Step size between consecutive sections was 1.5µm. In total 13 images were taken for each section, across 20.5µm. Each maximal image was composed of multiple sections to ensure optimum capture of labels.

ImageJ (Wayne Rasband, NIH) was used to determine numerical values representing the location of retrograde and anterograde labelling in temporal and sensory-motor cortex. The dorsoventral and medial-lateral distance (i.e. laminar location) of each Fluoro-Gold labelled cell in temporal cortex was measured from the rhinal sulcus and cortical surface respectively. The anterior-posterior location of each retrogradely labelled cell in temporal cortex was also recorded, in terms of distance (mm) from Bregma according to a stereotaxic atlas (Paxinos and Watson, 1998). This process was repeated for Fluoro-Ruby labelling. A similar acquisition of data was implemented for labelling in sensory-motor cortex, whereby the dorsoventral and medial-lateral distance of labels from the cortical surface was recorded. The anterior-posterior location of each label in sensory-motor cortex was also recorded, in terms of distance (mm) from Bregma.

Results

Fluoro-Gold labelling was found in areas of primary and secondary motor cortex (M1, M2), primary somatosensory cortex (jaw region and barrel field - S1J, S1BF), area 1 of cingulate cortex (Cg1), piriform cortex (Pir), perirhinal cortex (PRh - areas 35v, 35d, 36d, 36v), entorhinal cortex (Ent), primary auditory cortex (Au1), ventral secondary auditory cortex (AuV) and prefrontal regions. Fluoro-Ruby labelling was found in areas of M2, S1J, Cg1, S2, PRh, Ent, dorsal agranular insular cortex (AID) and prefrontal regions. The organisation of input and output connections were initially investigated at two anterior-posterior PFC locations separately (anterior (4.7mm from Bregma) and posterior (3.7mm from Bregma)). We proceeded to examine the connectivity across the whole investigated PFC region, from anterior to posterior, for connections from PFC to temporal and sensory-motor cortex.

Injections into anterior and posterior PFC

Fluoro-Gold injection sites into the anterior (bregma + 4.7mm) and posterior (bregma +3.7mm) aspect of PFC were observed in PL, VO, VLO and DLO anteriorly and in PL, IL, MO,VO, VLO, LO and AI posteriorly (Figure 1ii, iv). These injection sites were mostly confined to layers I-V/VI. No overlapping occurred between Fluoro-Ruby PFC injection sites.

Anterior PFC: There was some overlap seen between the Fluoro-Gold injection sites in PL (R28) and VO (R24). There was some minimal overlap between the Fluoro-Gold injections into VO and VLO (R24 and R17). Fluoro-Ruby injection sites into anterior PFC were observed in similar regions to the equivalent Fluoro-Gold injection sites, the spread of Fluoro-Ruby injections was consistently contained within the boundary of Fluoro-Gold counterparts.

Posterior PFC: The injection into PL (R27) spread across layers II-VI and overlapped slightly with the injections into VO and VLO. The injection into VO (R22) overlapped with the PL injection and spread into the PL region, however the majority of injected tracer was seen within the intended regions of VO and MO. The VLO injection site also spread beyond the intended region, however the majority of injected tracer remained within the boundaries of VLO and covered layers I-VI. The lateral injection site did not overlap with any other Fluoro-Gold injection sites and remained mostly within the cytoarchitectural region of LO and AI. All of the Fluoro-Ruby injection sites produced a smaller spread of tracer than the corresponding Fluoro-Gold injection sites.

Labelling following PFC tracer injections

Fluoro-Gold labelling*,* resultant from tracer injections into anterior (+4.7mm from Bregma) PFC (PL, VO, VLO and DLO) was found in regions of PRh (36v, 36d, 35d), Ent, AuV, Cg1, M2, M1, S1J and prefrontal regions (Figure 2i, Figure 3i). Fluoro-Ruby labelling resultant from tracer injections into the same co-ordinates in anterior PFC was found in regions of PRh (36v, 36d, 35d), Ent, Cg1, M2 and M1, as well as prefrontal regions (Figure 2iv, Figure 3iv).

Fluoro-Gold labelling, resultant from injections into posterior (+3.7mm from Bregma) PFC (PL, VO, VLO and AI) was found in regions of PRh (35v, 35d, 36v, 36d), Ent, AuV, Cg1, M2,

M1, S1J and prefrontal regions (Figure 2ii, Figure 3ii). Fluoro-Ruby labelling resultant from injections into posterior PFC (PL, VO, VLO and AI) was found in regions of PRh (35d, 36v, 36d), Ent, Cg1, M2 and M1, as well as prefrontal regions (Figure 2iv, Figure 3iv).

Immunofluorescent imaging of alpha-tubulin alongside Fluoro-Ruby labelling in temporal cortex indicated that the majority (70%) of Fluoro-Ruby labelling we observed in temporal cortex, as a result of injections into prefrontal cortex, was separate from the fluorescein labelled cell bodies (Figure 4). There was some evidence of double labelling of alpha tubulin and Fluoro-Ruby (Figure 4), approximately 30% of cases were found to have retrograde properties (Fluorescein and Fluoro-Ruby labelling was seen in the same location).

Organisation and distribution of connections from Anterior PFC to Temporal Cortex

The distribution of retrogradely labelled axon terminals in temporal cortex maintained a spatial order in terms of the corresponding Fluoro-Gold anterior PFC injection site. Moving from medial to lateral in PFC (from VO to DLO), projections were seen more posteriorly within temporal cortex (fig 5i).

The distribution of anterogradely labelling (from Fluoro-Ruby) in temporal cortex resultant from anterior PFC tracer injections was less widespread than the corresponding retrograde labelling (from Fluoro-Gold) (Figure 5iii). The distribution and ordering of Fluoro_Ruby connections also differed to the distribution of Fluoro-Gold labelling. Although the labelling appeared in the same extent of temporal cortex the Fluoro-Ruby injections produced orbital projections (moving medial to lateral, VO-VLO) at broadly progressively anterior locations within temporal cortex. The clearest differences in the locations of anterograde and retrograde labelling resulted from injections into both VO and DLO.

Organisation and distribution of Connections from Posterior PFC to Temporal Cortex

The distribution of retrogradely labelled cells within temporal cortex maintained a spatial order according to the corresponding Fluoro-Gold posterior PFC injection sites. Moving from medial to lateral in posterior PFC (from VO to AI), labelling was seen at progressively anterior locations within temporal cortex. For example, retrogradely labelled cells resultant from VO injections were most posteriorly located and VLO injections produced labelling in more anteriorly located temporal cortex sites (fig.5ii).

The distribution of anterogradely labelled axon terminals maintained a spatial order according to Fluoro-Ruby posterior PFC injection sites which was similar to that for retrograde labelling (Figure 5iv). Moving from medial to lateral in posterior PFC (VO to AI), anterograde labels in temporal cortex occurred at increasingly anterior locations (fig.5iv). In contrast to anterior PFC, injections at equivalent mediolateral injections (i.e.1.2, 2.2 or 3.3mm lateral to the midline) produced similar locations for anterograde and retrograde labelling within temporal cortex.

Organisation and distribution of Connections from Anterior PFC to Sensory-motor cortex

The distribution of retrogradely labelled cells in sensory-motor cortex maintained an overall spatial order according to the corresponding (Fluoro-Gold) anterior PFC injection sites (VO, VLO and DLO). Moving from medial to lateral in PFC (from VO to DLO), projections were seen more posteriorly within temporal cortex (fig 6i).

The distribution of anterogradely labelled axon terminals in sensory-motor cortex maintained a different spatial order in terms of the corresponding Fluoro-Ruby anterior PFC injection site (Fig.6iii). Moving from medial to lateral in PFC (from VO to DLO), this time projections were seen at increasingly anterior locations. For example, projections from VLO were seen at more anterior locations compared to those arising from VO. The VO and DLO injection sites had the most different locations of anterograde and retrograde labelling within temporal cortex.

Organisation and distribution of connections from Posterior PFC to Sensory-motor cortex

The distribution of retrogradely labelled cells within sensory-motor cortex maintained some spatial ordering according to the corresponding Fluoro-Gold injection sites in posterior PFC. Moving laterally in PFC from VO to AI: projections were seen more anteriorly within temporal cortex (fig 6ii). Here labelling from the injection into VO and AI is located anteriorly to that resulting from injection into VO.

The distribution of anterogradely labelled axon terminals in sensory-motor cortex maintained a spatial order corresponding to Fluoro-Ruby posterior PFC injection sites which resembled that of Fluoro-Gold labelling. As PFC injection sites move from medial to lateral (VO to AI),

labelling in sensory-motor cortex occur at increasingly anterior locations (fig.6iv). In contrast to anterior PFC, the VO and AI injection sites had similar locations of anterograde and retrograde labelling within temporal cortex.

We also plotted the location of the anterograde and retrograde tracer in three axes of orientation (dorsoventral, anterior-posterior and mediolateral) within both the temporal and sensory-motor cortex regions (see Figures 7-10). The location data within temporal cortex is shown following anterior (Figure 7) and posterior (Figure 8) PFC injections. The anterograde and retrograde labelling shows locational differences in temporal cortex for both anterior and posterior injections however the clearest difference appears in the plotting along the anterior-posterior axis following anterior PFC injections (Figure 7ii): note the difference in retrograde and anterograde positions after injections Ba and Da. By contrast the difference in anterograde and retrograde labelling following injections into posterior PFC were much less marked in the anterior-posterior axis (Figure 8ii).

The location data within sensory-motor cortex following anterior and posterior PFC injections is shown in figures 9 and 10 respectively. Again the anterograde and retrograde labelling shows locational differences in sensory-motor cortex for both anterior and posterior injections, and like the temporal cortex results, note the difference in positions of anterograde and retrograde labels in the anterior-posterior axis following anterior PFC injections (Figure 9ii – injections Aa, Ba and Da). As was the case for the temporal cortex labelling, the difference in anterograde and retrograde labelling following injections into posterior PFC was less marked in the anterior-posterior axis (Figure 10ii).

Discussion

Our study is the first to provide detailed analysis of how the ordering of connections changes within anterior and posterior portions of rat PFC. Further, we report that there are changes in the ordering of connections to both temporal and sensory motor cortices at anterior or posterior levels of rat prefrontal cortex.

Methodological and Interpretative Considerations

Our results have shown that the FG injections produced retrograde labelling and our FR injections primarily produced anterograde labelling. For FR labelling we base this judgement

on the majority of labelling not co-localising with alpha-tubulin (a cytosplasmic marker). We used relatively large tracer injections (of 100nl FG and 100nl FR) because this produced a consistent and repeatable injection volume that ensured significant labelling within the projection sites (i.e. connected regions). We cannot rule out some spread to fibers of passage. The size of the tracer injections inevitably also meant that tracer was not usually confined to just one sub-region of PFC, in the case of PL injections there was also some spread into secondary motor cortex. Here we aimed to look at how connectional architecture changes at anterior and posterior PFC levels however the changing shape and architecture of PFC in the A-P axis provided limitations to the study (see below for a detailed discussion).

Organisation of Connections from Anterior and Posterior Prefrontal Cortex to Temporal Cortex

In this study we observed apparent ordering of connections in the location of anterograde and retrograde connections from both anterior and posterior PFC and to both temporal and sensory-motor cortex.

In addition we found that for *anterior PFC* this ordering of connections differed for the anterograde and retrograde labels employed. In other words, the distribution of retrograde and anterograde tracer occurred in different sub-regions of temporal cortex. The differences were most notable following injections into medial orbital cortex (i.e. VO) or following injections into DLO (i.e lateral PFC). This is of interest because it produced a very similar ordering and distribution of labels to that found following tracer injections into a 'central', coronal portion of PFC (Bedwell et al, 2015), located at the equivalent coronal level of bregma +4.2mm (a coronal level half way between the 2 sections in figure 1 of the present study). Specifically Fluoro-Gold and Fluoro-Ruby injections into VO, VLO and DLO at this level produced labelling in correspondingly similar positions within temporal and sensory-motor cortex. This study also found that the distribution of anterograde and retrograde labels did not correspond (particularly in the case of VO and DLO).

Further to this, we found that for the posterior PFC region we studied the ordering and distribution of Fluoro-Gold (retrograde) and Fluoro-Ruby (anterograde) labels was much more similar. In the case of posterior PFC, VO (medial orbital) and AI (lateral PFC) labelling of retrograde and anterograde labels occurred in relatively similar locations (in comparison to equivalent distributions following equivalent anterior medial orbital (VO) and lateral orbital (DLO) injections). There could be several possible reasons for this dissociation between anterior and posterior PFC. The first and most plausible reason is that the cytoarchitectural

regions compared are not equivalent. The most lateral injections made into the anterior PFC occupied DLO, at the posterior PFC level studied the most lateral injection occupied predominantly agranular insular cortex. This may explain the disparity seen in terms of different locations of retrograde label (DLO versus AI). By examining the injection locations of the most medial orbital injections (anterior versus posterior) it is also clear that, due to the changing shape of PFC subdivisions, tracer occupied different subdivisons (anterior PFC: predominantly VO and MO; posterior PFC: VO, MO, IL, PL). These cytoarchitectural differences in terms of injection site may help to explain the apparent differences, notably in relation to the distribution of retrograde tracer. Another possible interpretation for these differences is that there is a broad organisational difference within rat prefrontal cortex, where anterior and central regions of PFC contain many non-reciprocal connections and posterior PFC connections are more reciprocal in nature.

Organisation of Connections from Anterior and Posterior Prefrontal Cortex to the Sensory-Motor Cortex

We observed strong connections between prefrontal cortex and the sensory-motor cortex. A previous study has reported connections between rat orbital cortex and the cingulate cortex and secondary somatic sensory motor area (Reep et al., 1996). The rat precentral medial area is also known to connect to somatosensory cortex (Conde et al., 1995). In primates S1 receives afferent connections from premotor areas (Cerkevich et al., 2014). Projections from the sensory-motor cortex region to the different PFC regions frequently arose from distinct cortical layers within somatosensory cortex, this resembled a similar pattern of projections from the striatum to the medial PFC described previously (Gabbott et al., 2005) and was in agreement with our previous report concerning the connections of central PFC (Bedwell et al 2014). Within the two coronal levels studied here we saw ordering prominent within the connections to sensory-motor cortex of the orbital region of cortex. In common with the temporal cortex connections, the ordering of sensory-motor cortex-PL connections did not fit within the ordering scheme of orbital connections (again for both FG and FR labels). A similar pattern of labelling was observed in the PFC-sensory-motor connections as was seen in the PFC-temporal connections. Here the ordering of anterograde and retrograde connections (arising from the orbital region) differed for equivalent injections in the anterior level. However at the posterior coronal level the ordering observed was similar for retrograde and anterograde labelling seen within temporal cortex. Similarly at the level of individual injection sites this meant that for posterior PFC, VO (medial orbital) and AI (lateral PFC) labelling of retrograde and anterograde labels occurred in

relatively similar locations (in comparison to equivalent distributions following equivalent anterior medial orbital (VO) and lateral orbital (DLO) injections). The reasons for this disparity are discussed in the preceding section on PFC-temporal cortex connections.

Our analysis also shows that, in general, the distributional spread of connections became more widespread in the target regions following more posteriorly located PFC injections (this was particularly clear in the spread of connections to sensory-motor cortex shown in figure 6). This was the case for both anterograde and retrograde connections. This indicates that there was a change in the organisational patterns of divergence and convergence as we move from anterior to posterior PFC. This additional change in the organisation of connections could have important implications for key processing characteristics within PFC circuits.

Conclusions

Clearly the organisation of cortical connections has important functional consequences in terms of both physiological organisation and function. The topology and topography of cortical connections to sensory cortices supports (1) the existence of both sensory and cognitive maps and (2) important perceptual functions such as visual feedback (Wang et al., 2006) and attention (Tootell et al., 1982). Our finding provides insight to the complex ordering seen in prefrontal cortex. Some functional studies of PFC have reported changes in cortical connectivity in areas of PFC. One study described how responses to happy or sad faces modulated unidirectional connections or bi-directional connections between orbitofrontal cortex and the fusiform gyrus in humans (Goulden et al., 2012). It is possible that the changes in ordered connections seen along in the anterior-posterior axis in the present study may be related to the functional connectivity described above. Whatever the functional implications, these findings should promote further investigations into the anatomy and organisation of this important cortical region.

References

Agster KL, Burwell RD (2013) Hippocampal and subicular efferents and afferents of the perirhinal, postrhinal, and entorhinal cortices of the rat. Behav Brain Res (Netherlands) 254:50-64.

Alvarez JA, Emory E (2006) Executive function and the frontal lobes: A meta-analytic review. Neuropsychol Rev (United States) 16:17-42.

Arnault P, Roger M (1990) Ventral temporal cortex in the rat: Connections of secondary auditory areas Te2 and Te3. J Comp Neurol (UNITED STATES) 302:110-123.

Aronoff R, Matyas F, Mateo C, Ciron C, Schneider B, Petersen CC (2010) Long-range connectivity of mouse primary somatosensory barrel cortex. Eur J Neurosci (France) 31:2221-2233.

Bedwell SA, Billett EE, Crofts JJ, Tinsley CJ (2014) The topology of connections between rat prefrontal, motor and sensory cortices. Front Syst Neurosci (Switzerland) 8:177.

Bedwell SA, Billett EE, Crofts JJ, MacDonald DM, Tinsley CJ (2015) The topology of connections between rat prefrontal and temporal cortices. Front Syst Neurosci (Switzerland) 9:80.

Berendse HW, Galis-de Graaf Y, Groenewegen HJ (1992) Topographical organization and relationship with ventral striatal compartments of prefrontal corticostriatal projections in the rat. J Comp Neurol (UNITED STATES) 316:314-347.

Burwell RD, Witter MP, Amaral DG (1995) Perirhinal and postrhinal cortices of the rat: A review of the neuroanatomical literature and comparison with findings from the monkey brain. Hippocampus (UNITED STATES) 5:390-408.

491 Cerkevich CM, Qi HX, Kaas JH (2014) Corticocortical projections to representations of the
492 teeth, tongue, and face in somatosensory area 3b of macaques. J Comp Neurol (United
493 States) 522:546-572.

494 Conde F, Maire-Lepoivre E, Audinat E, Crepel F (1995) Afferent connections of the medial
495 frontal cortex of the rat. II. cortical and subcortical afferents. J Comp Neurol (UNITED
496 STATES) 352:567-593.

497 Delatour B, Witter MP (2002) Projections from the parahippocampal region to the
498 prefrontal cortex in the rat: Evidence of multiple pathways. Eur J Neurosci (France)
499 15:1400-1407.

500 Frysztak RJ, Neafsey EJ (1994) The effect of medial frontal cortex lesions on
501 cardiovascular conditioned emotional responses in the rat. Brain Res (NETHERLANDS)
502 643:181-193.

503 Fuster JM (2001) The prefrontal cortex--an update: Time is of the essence. Neuron (United
504 States) 30:319-333.

505 Gabbott PL, Warner TA, Jays PR, Salway P, Busby SJ (2005) Prefrontal cortex in the rat:
506 Projections to subcortical autonomic, motor, and limbic centers. J Comp Neurol (United
507 States) 492:145-177.

508 Gattass R, Nascimento-Silva S, Soares JG, Lima B, Jansen AK, Diogo AC, Farias MF,
509 Botelho MM, Mariani OS, Azzi J, Fiorani M (2005) Cortical visual areas in monkeys:
510 Location, topography, connections, columns, plasticity and cortical dynamics.
511 Philosophical Transactions of the Royal Society of London 360:709-31.

512 Goulden N, McKie S, Thomas EJ, Downey D, Juhasz G, Williams SR, Rowe JB, Deakin
513 JF, Anderson IM, Elliott R (2012) Reversed frontotemporal connectivity during emotional
514 face processing in remitted depression. Biol Psychiatry (United States) 72:604-611.

515 Henry EC, Catania KC (2006) Cortical, callosal, and thalamic connections from primary
516 somatosensory cortex in the naked mole-rat (heterocephalus glaber), with special
517 emphasis on the connectivity of the incisor representation. Anat Rec A Discov Mol Cell
518 Evol Biol (United States) 288:626-645.

519 Hoover WB, Vertes RP (2011) Projections of the medial orbital and ventral orbital cortex in
520 the rat. J Comp Neurol (United States) 519:3766-3801.

521 Kim J, Ghim JW, Lee JH, Jung MW (2013) Neural correlates of interval timing in rodent
522 prefrontal cortex. J Neurosci (United States) 33:13834-13847.

523 Kolb B (1984) Functions of the frontal cortex of the rat: A comparative review. Brain Res
524 (NETHERLANDS) 320:65-98.

525 Kondo H, Witter MP (2014) Topographic organization of orbitofrontal projections to the
526 parahippocampal region in rats. J Comp Neurol (United States) 522:772-793.

527 Krettek JE, Price JL (1977) The cortical projections of the mediodorsal nucleus and
528 adjacent thalamic nuclei in the rat. J Comp Neurol (UNITED STATES) 171:157-191.

529 Narayanan NS, Laubach M (2009) Delay activity in rodent frontal cortex during a simple
530 reaction time task. J Neurophysiol (United States) 101:2859-2871.

531 Narayanan NS, Laubach M (2008) Neuronal correlates of post-error slowing in the rat
532 dorsomedial prefrontal cortex. J Neurophysiol (United States) 100:520-525.

533 Narayanan NS, Laubach M (2006) Top-down control of motor cortex ensembles by
534 dorsomedial prefrontal cortex. Neuron (United States) 52:921-931.

535 Neafsey EJ (1990) Prefrontal cortical control of the autonomic nervous system: Anatomical
536 and physiological observations. Prog Brain Res (NETHERLANDS) 85:147-65; discussion
537 165-6.

538 Olson CR, Musil SY (1992) Topographic organization of cortical and subcortical
539 projections to posterior cingulate cortex in the cat: Evidence for somatic, ocular, and
540 complex subregions. The Journal of Comparative Neurology 324:237-60.

541 Paxinos G, Watson C (1998) The rat brain in stereotaxic coordinates. San Diego, CA:
542 Academic Press.

543 Porter LL, White EL (1983) Afferent and efferent pathways of the vibrissal region of
544 primary motor cortex in the mouse. J Comp Neurol (UNITED STATES) 214:279-289.

545 Reep RL, Corwin JV, King V (1996) Neuronal connections of orbital cortex in rats:
546 Topography of cortical and thalamic afferents. Exp Brain Res (GERMANY) 111:215-232.

547 Schilman EA, Uylings HB, Galis-de Graaf Y, Joel D, Groenewegen HJ (2008) The orbital
548 cortex in rats topographically projects to central parts of the caudate-putamen complex.
549 Neurosci Lett (Ireland) 432:40-45.

550 Schoenbaum G, Esber GR (2010) How do you (estimate you will) like them apples?
551 integration as a defining trait of orbitofrontal function. Curr Opin Neurobiol (England)
552 20:205-211.

553 Schoenbaum G, Roesch M (2005) Orbitofrontal cortex, associative learning, and
554 expectancies. Neuron (United States) 47:633-636.

555 Sesack SR, Deutch AY, Roth RH, Bunney BS (1989) Topographical organization of the
556 efferent projections of the medial prefrontal cortex in the rat: An anterograde tract-tracing
557 study with phaseolus vulgaris leucoagglutinin. J Comp Neurol (UNITED STATES)
558 290:213-242.

559 Smith NJ, Horst NK, Liu B, Caetano MS, Laubach M (2010) Reversible inactivation of rat
560 premotor cortex impairs temporal preparation, but not inhibitory control, during simple
561 reaction-time performance. Front Integr Neurosci (Switzerland) 4:124.

562 Stalnaker TA, Cooch NK, Schoenbaum G (2015) What the orbitofrontal cortex does not
563 do. Nat Neurosci (United States) 18:620-627.

564 Taren AA, Venkatraman V, Huettel SA (2011) A parallel functional topography between
565 medial and lateral prefrontal cortex: Evidence and implications for cognitive control. J
566 Neurosci (United States) 31:5026-5031.

567 Tootell RB, Silverman MS, Switkes E, De Valois RL (1982) Deoxyglucose analysis of
568 retinotopic organization in primate striate cortex. Science (UNITED STATES) 218:902-904.

569 Van De Werd HJ, Uylings HB (2008) The rat orbital and agranular insular prefrontal
570 cortical areas: A cytoarchitectonic and chemoarchitectonic study. Brain Struct Funct
571 (Germany) 212:387-401.

572 Vertes RP (2006) Interactions among the medial prefrontal cortex, hippocampus and
573 midline thalamus in emotional and cognitive processing in the rat. Neuroscience (United
574 States) 142:1-20.

575 Vertes RP (2004) Differential projections of the infralimbic and prelimbic cortex in the rat.
576 Synapse (United States) 51:32-58.

577 Wang W, Jones HE, Andolina IM, Salt TE, Sillito AM (2006) Functional alignment of
578 feedback effects from visual cortex to thalamus. Nat Neurosci (United States) 9:1330-
579 1336.

580
581

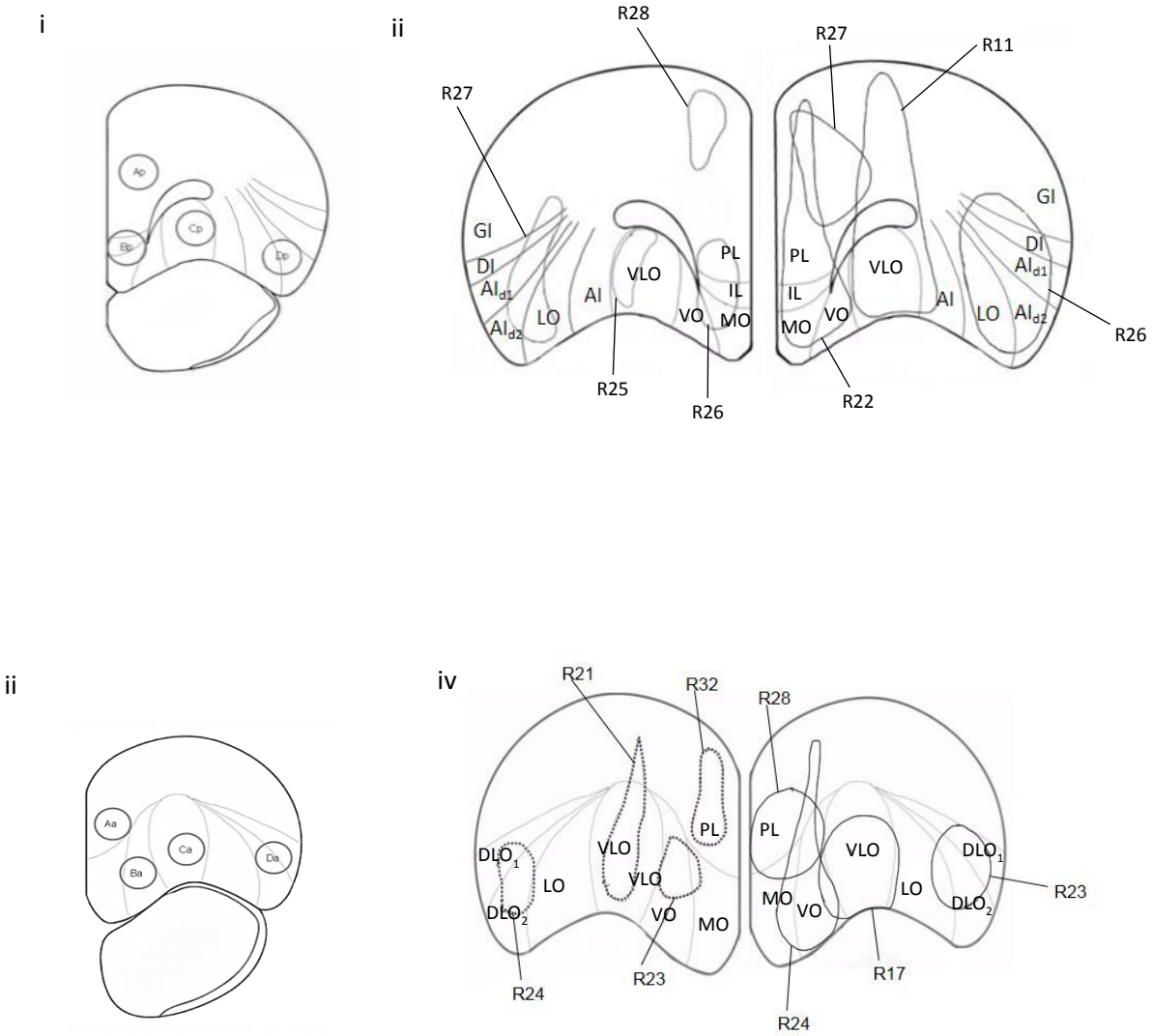

Figure 1. Tracer injections into posterior and anterior prefrontal regions. **(i)** Coronal section of posterior PFC (+3.7mm anterior to Bregma) showing the cytoarchitectural boundaries of PFC sub-regions according to Van de Werd & Uylings (2008), depicting intended sites of tracer injections; PL (Ap), VO (Bp), VLO (Cp) and AI (Dp), with 1mm separation. **(ii)** Representations of Fluoro-Ruby (100nl) (R25, R26, R27, R28 (broken line) injection sites in PL (R28), VO (R26), VLO (R25) and AI (R27), in the right hemisphere. Representations of Fluoro-Gold (100nl) (R11, R22, R26, R27 (solid line)) injection sites in PL (R27), VO (R22), VLO (R11) and DLO (R26), in the left hemisphere. **(iii)** Coronal section of anterior PFC (+4.7mm anterior to Bregma) showing the cytoarchitectural boundaries of PFC sub-regions according to Van de Werd & Uylings (2008), depicting sites of tracer injections; PL (Aa), VO (Ba), VLO (Ca) and DLO (Da), with 1mm separation. **(iv)** Representations of Fluoro-Ruby (100nl) (R21, R23, R24, R32 (broken line)) injection sites in anterior PL (R32), VO (R23), VLO (R21) and DLO (R24) in the right hemisphere. Representations of Fluoro-Gold (100nl) (R17, R23, R24, R28 (solid line) injection sites in anterior PL (R28), VO (R24), VLO (R17) and DLO (R23) in the left hemisphere. The diagrams represent an amalgamation of injection sites from the animals indicated by the 'R' number.

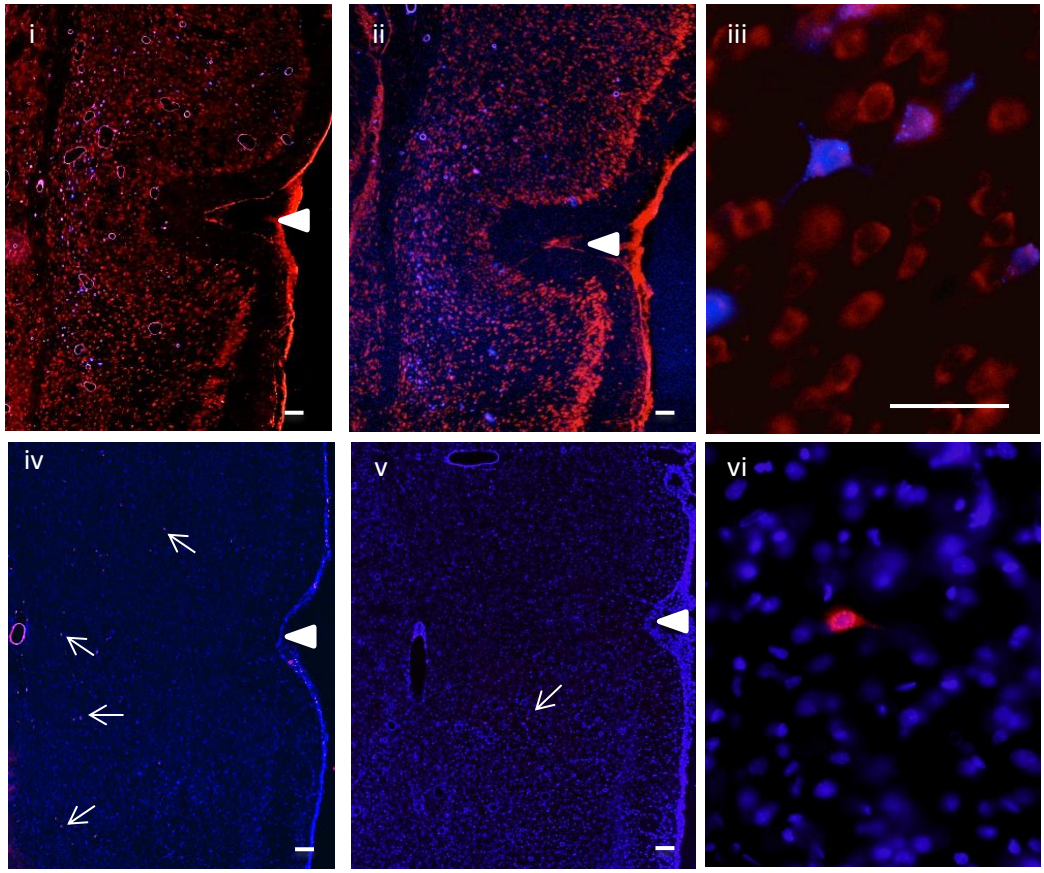

Figure 2. Coronal sections showing retrogradely labelled cells (blue) in temporal cortex produced by injections of 100nl Fluoro-Gold into **(i)** anterior VO (R24), **(ii)** posterior VO (R22) (x4) and **(iii)** high magnification photomicrograph showing posterior PL (R27) (x20). Propidium Iodide was used to stain the background cells (red). Coronal sections showing anterograde labelling (red) in temporal cortex produced by 100nl Fluoro-Ruby injections into **(iv)** anterior VO (R23), **(v)** posterior VO (R26) (x4) and **(vi)** high magnification photomicrograph showing Fluoro-Ruby labelling from injection into posterior VLO (R25) (x20). DAPI was used to stain the background cells (blue). The triangles denote the location of the rhinal sulcus. Arrows indicate locations of Fluoro-Ruby labelling. Scale bars = 100μm.

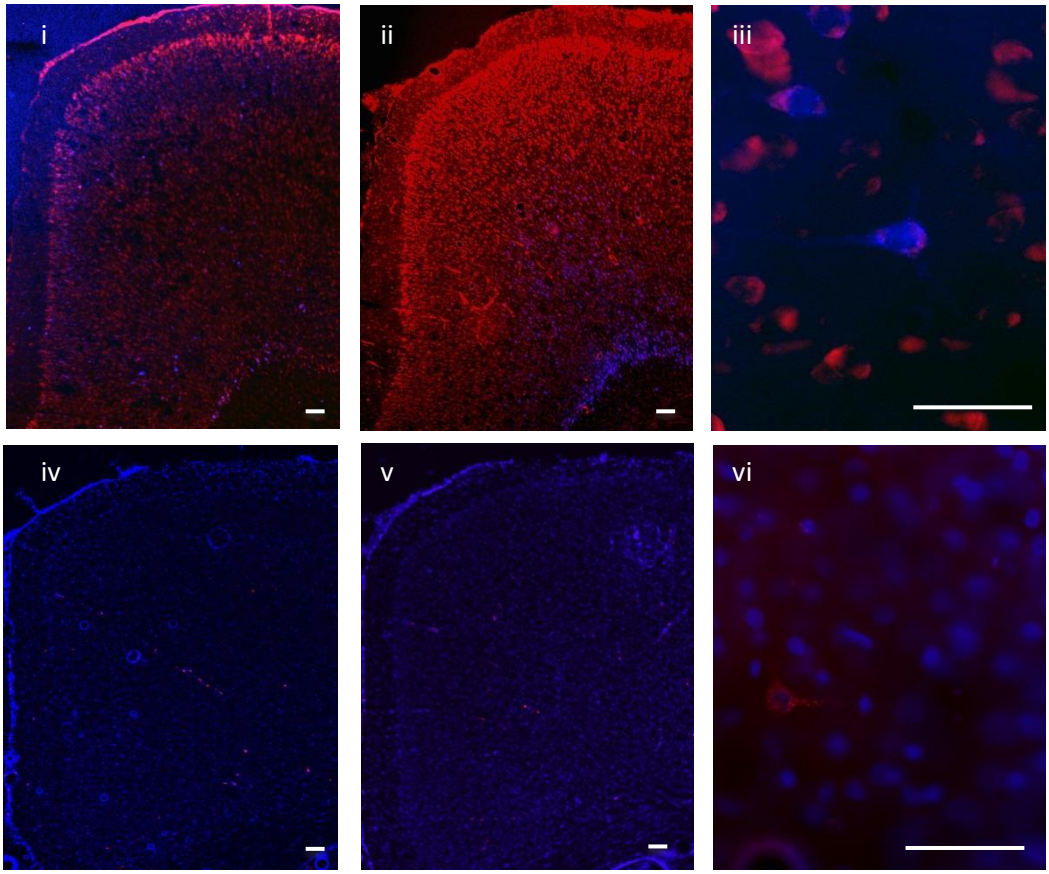

Figure 3. Coronal sections showing retrogradely labelled cells (blue) in sensory-motor cortex produced by injections of 100nl Fluoro-Gold into **(i)** anterior VO (R24), **(ii)** posterior VO (R22) (x4) and **(iii)** high magnification photomicrograph showing anterior VO (R24) (x20). Propidium Iodide was used to stain the background cells (red). Coronal sections showing anterograde labelling (red) in temporal cortex produced by 100nl Fluoro-Ruby injections into **(iv)** anterior VO (R23) (x4), **(v)** posterior VO (R26) (x4) and **(vi)** high magnification photomicrograph showing posterior VO (R26) (x20). DAPI was used to stain the background cells (blue). Scale bars = 100µm.

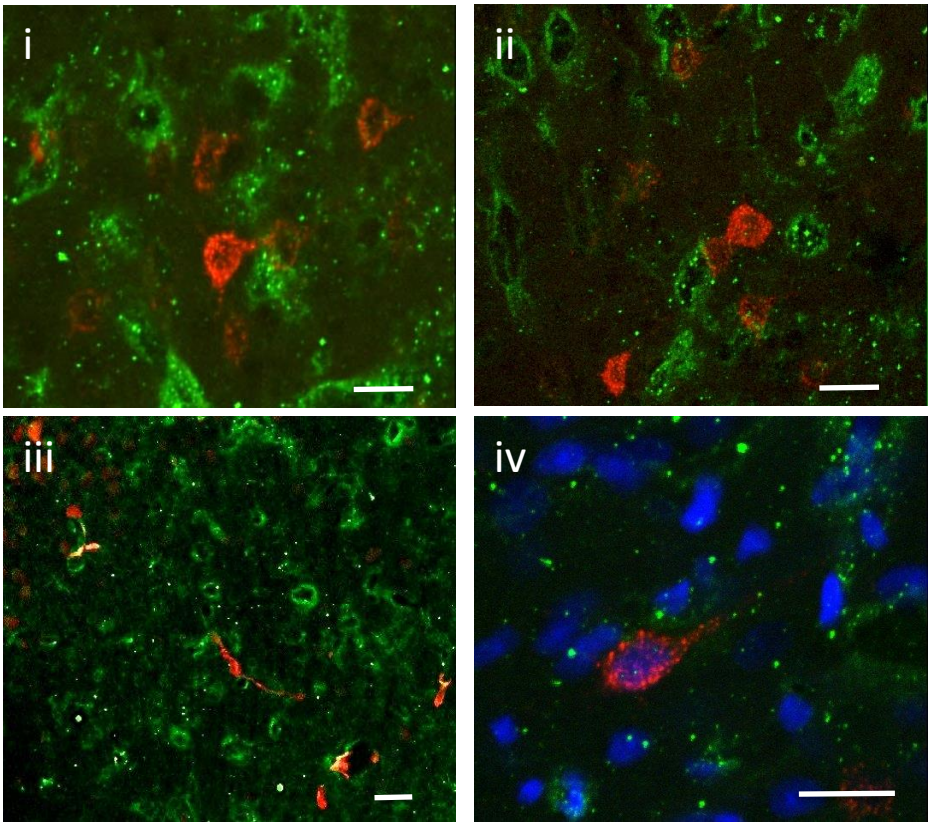

Figure 4. (i, ii & iii) Images of temporal cortex depicting fluorescently (fluorescein) labelled alpha tubulin (green) and Fluoro-Ruby labelling (red) resultant from (100nl) injection into PFC (Animal ID = R39). (iv) Image of temporal cortex depicting fluorescently labelled alpha tubulin (green), DAPI labelled nuclei (blue) and Fluoro-Ruby labelling (red) resultant from (100nl) injection into PFC. Dual-labelling of Fluoro-Ruby and Fluorescein (alpha tubulin) is shown by yellow fluorescence (iii). Scale bars = 20µm.

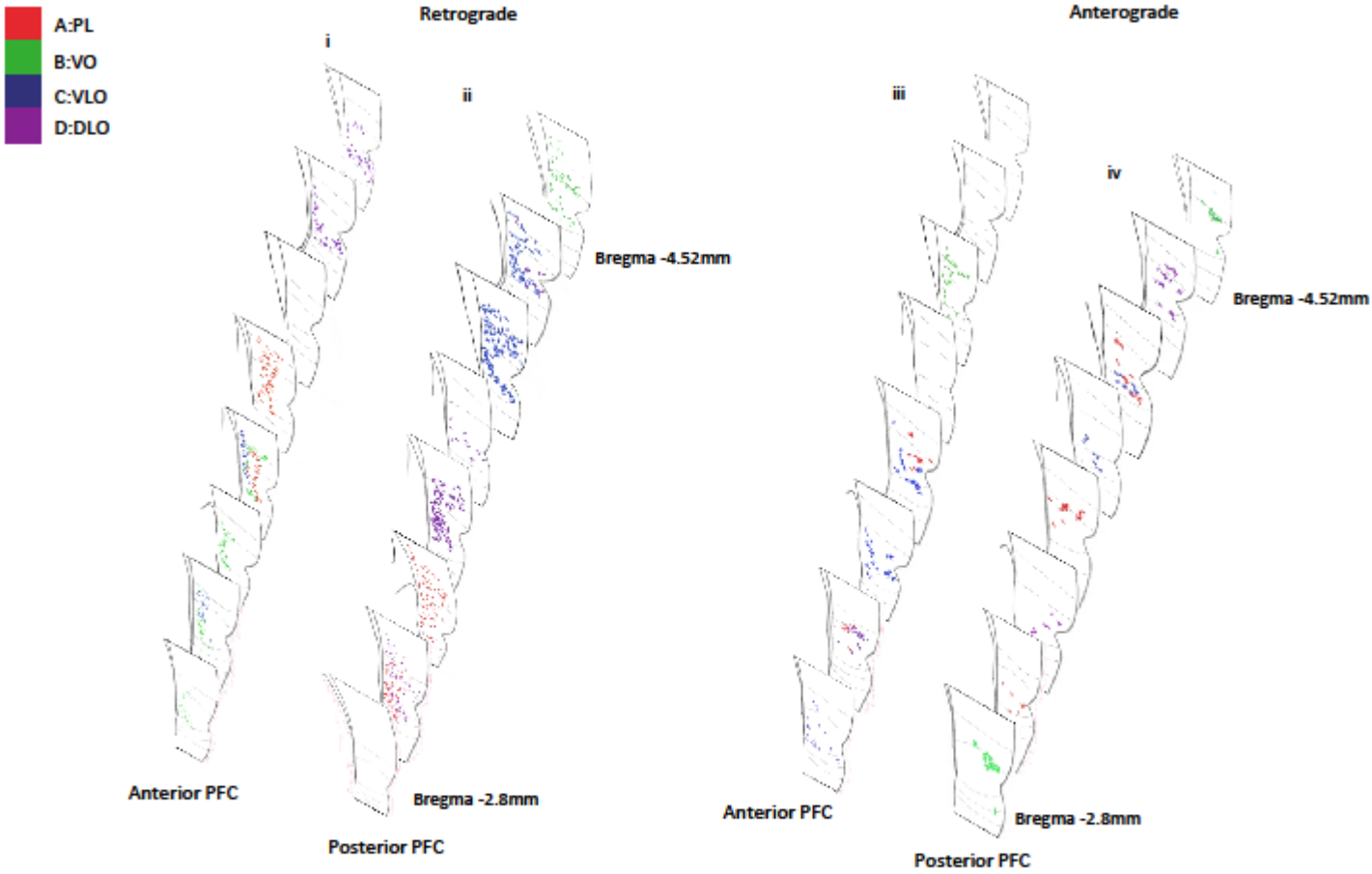

Figure 5. Diagram representing both retrograde (Fluoro-Gold) and anterograde (Fluoro-Ruby) projections to temporal cortex arising from tracer injections into the anterior and posterior PFC. **(i)** retrograde labelling in temporal cortex produced by Fluoro-Gold (100nl) injections into anterior PFC and **(ii)** posterior PFC. **(iii)** anterograde labelling in temporal cortex produced by Fluoro-Ruby (100nl) injections into anterior PFC and **(iv)** posterior PFC. The diagrams represent an amalgamation of injection sites from the animals included in the study.

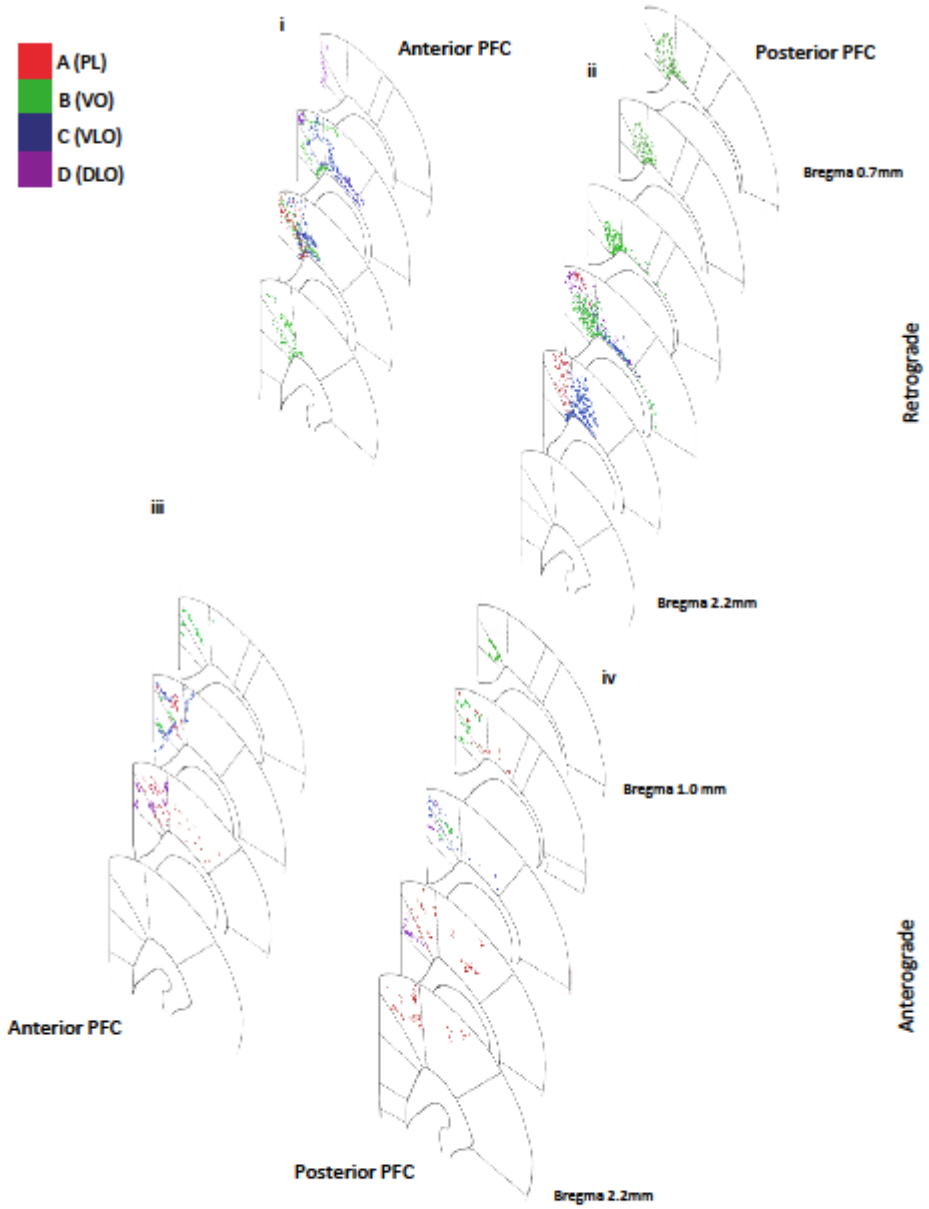

Figure 5. Diagram representing both retrograde (Fluoro-Gold) and anterograde (Fluoro-Ruby) projections to sensory-motor cortex arising from tracer injections into the anterior and posterior PFC. **(i)** retrograde labelling in sensory-motor produced by Fluoro-Gold (100nl) injections into anterior PFC and **(ii)** posterior PFC. **(iii)** anterograde labelling in sensory-motor cortex produced by Fluoro-Ruby (100nl) injections into anterior PFC and **(iv)** posterior PFC. The diagrams represent an amalgamation of injection sites from the animals included in the study.

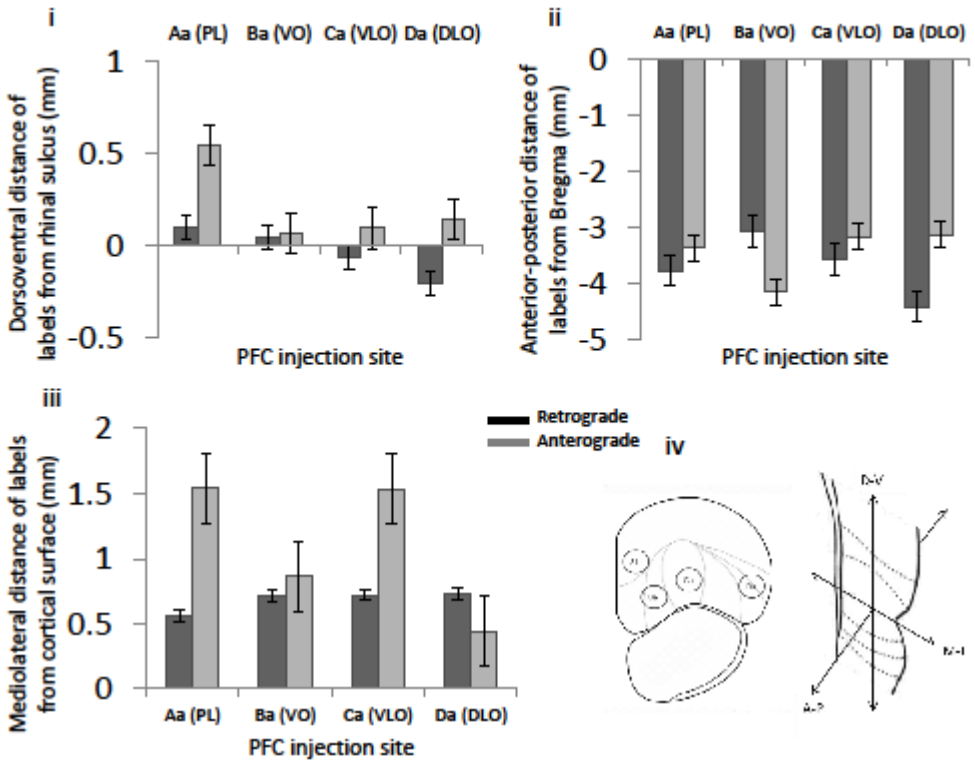

Figure 7. The mean effect of anterior PFC injection site on the location of retrograde and anterograde labels in temporal cortex in (i) dorsoventral, (ii) anterior-posterior and (iii) mediolateral axes. (iv) Coronal cross section of PFC indicating the position of four injection sites within PFC: Prelimbic (injection Aa), Ventral Orbital (injection Ba), Ventrolateral Orbital (injection Ca) and Dorsal Lateral Orbital (injection Da), coronal cross section of temporal cortex, depicting the three dimensions in which the locations of labelled cells were recorded. Error bars = standard error.

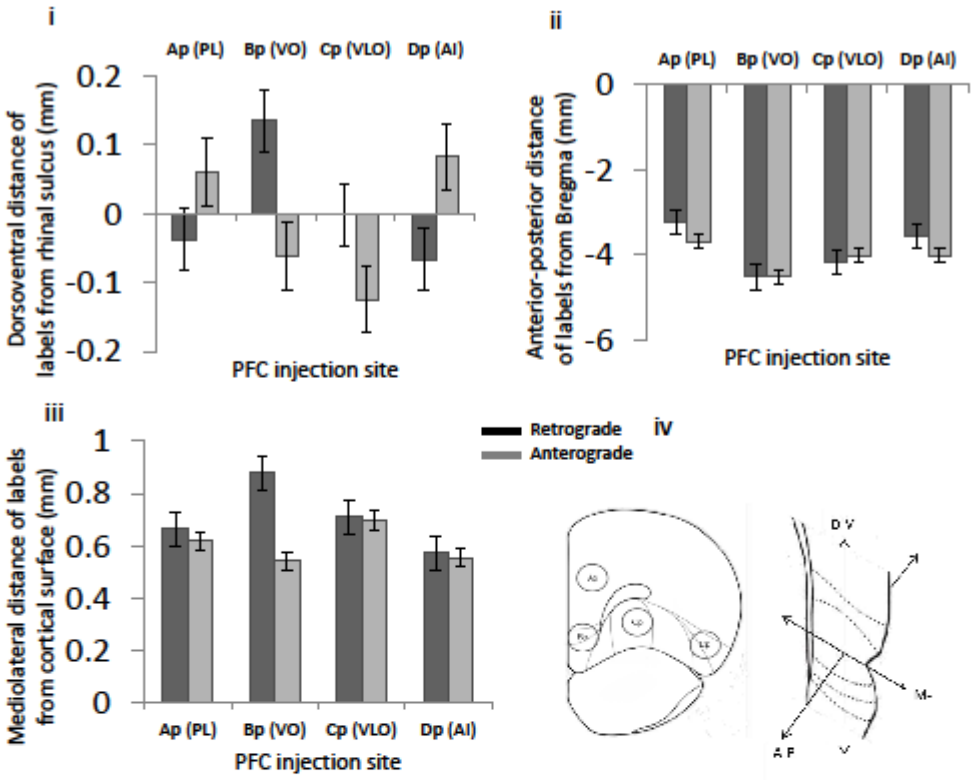

Figure 8. The mean effect of posterior PFC injection site on the location of retrograde and anterograde labels in temporal cortex in (i) dorsoventral, (ii) anterior-posterior and (iii) mediolateral axes. (iv) Coronal cross section of PFC indicating the position of four injection sites within PFC: Prelimbic (injection Ap), Ventral Orbital (injection Bp), Ventrolateral Orbital (injection Cp) and Agranular Insular cortex (injection Dp), coronal cross section of temporal cortex, depicting the three dimensions in which the locations of labelled cells were recorded. Error bars = standard error.

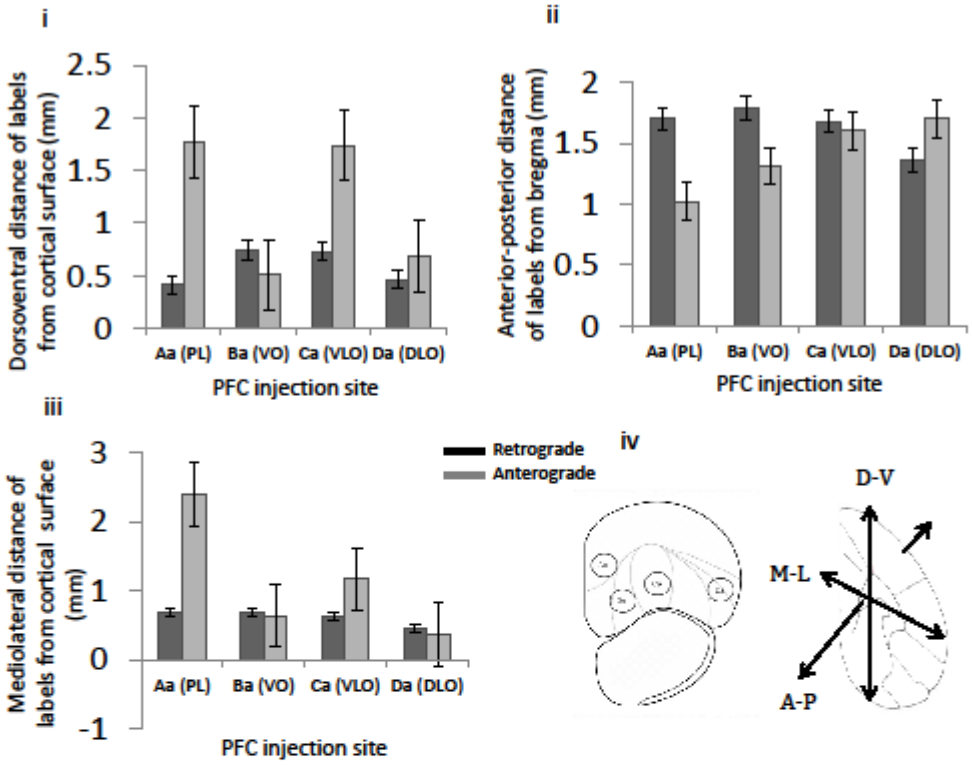

Figure 9. The mean effect of anterior PFC injection site on the location of retrograde and anterograde labels in sensory-motor cortex in (i) dorsoventral, (ii) anterior-posterior and (iii) mediolateral axes. (iv) Coronal cross section of PFC indicating the position of four injection sites within PFC: Prelimbic (injection Aa), Ventral Orbital (injection Ba), Ventrolateral Orbital (injection Ca) and Dorsal Lateral Orbital (injection Da), coronal cross section of sensory-motor cortex, depicting the three dimensions in which the locations of labelled cells were recorded. Error bars = standard error.

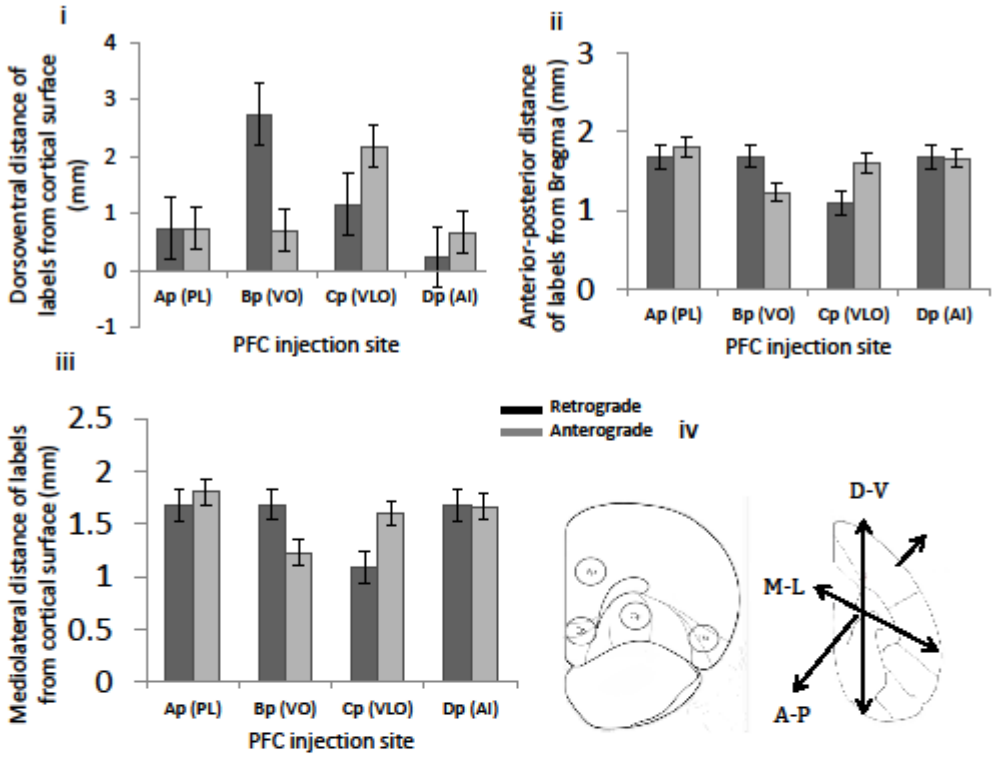

Figure 10. The mean effect of posterior PFC injection site on the location of retrograde and anterograde labels in sensory-motor cortex in (i) dorsoventral, (ii) anterior-posterior and (iii) mediolateral axes. (iv) Coronal cross section of PFC indicating the position of four injection sites within PFC: Prelimbic (injection Ap), Ventral Orbital (injection Bp), Ventrolateral Orbital (injection Cp) and Agranular Insular cortex (injection Dp), coronal cross section of sensory-motor cortex, depicting the three dimensions in which the locations of labelled cells were recorded. Error bars = standard error.

Rat ID	Hemisphere (L/R)	Tracer	AP	ML	Height
11	Left	Fluoro-Gold	3.2	2.2	3.2
17	Left	Fluoro-Gold	4.2	2.2	3.2
21	Right	Fluoro-Ruby	4.2	2.2	3.2
22	Left	Fluoro-Gold	3.2	1.2	3.2
23	Right	Fluoro-Ruby	4.2	1.2	3.2
23	Left	Fluoro-Gold	4.2	3.2	3.2
24	Right	Fluoro-Ruby	4.2	3.2	3.2
24	Left	Fluoro-Gold	4.2	1.2	3.2
25	Right	Fluoro-Ruby	3.2	2.2	3.2
26	Left	Fluoro-Gold	3.2	3.2	3.2
26	Right	Fluoro-Ruby	3.2	1.2	3.2
27	Right	Fluoro-Ruby	3.2	3.2	3.2
27	Left	Fluoro-Gold	3.2	1.2	2.4
28	Left	Fluoro-Gold	4.2	1.2	2.4
28	Right	Fluoro-Ruby	3.2	1.2	2.4
32	Right	Fluoro-Ruby	4.2	1.2	2.4
37	Right	Fluoro-Ruby	4.2	2.2	1.0
38	Right	Fluoro-Ruby	4.2	3.2	1.0
39	Left	Fluoro-Ruby	3.7	1.2	3.2

Table 1. Stereotaxic location of tracer injections used in the statistical analyses for each individual rat. Stereotaxic location in terms of anterior-posterior (AP) distance with respect to bregma (these reflect the surgical stereotaxic coordinates rather than the histological coordinates confirmed later, which were slightly anterior), medial lateral (ML) distance with respect to bregma and height with respect to the cortical surface (all in mm). The tracer type and hemisphere is also provided.